catalysts

Article

Polymer-Supported Dioxidovanadium(V) Complex-Based Heterogeneous Catalyst for Multicomponent Biginelli Reaction Producing Biologically Active 3,4-Dihydropyrimidin-2-(1*H*)-ones

Mannar R. Maurya *, Akhil Patter, Devesh Singh and Kaushik Ghosh

Department of Chemistry, Indian Institute of Technology Roorkee, Roorkee 247667, India
* Correspondence: m.maurya@cy.iitr.ac.in

Abstract: Dioxidovanadium(V) complex [V^VO_2(sal-aebmz)] (**1**) (where Hsal-aebmz = Schiff base derived from the condensation of salicylaldehyde and 2-aminoethylbenzimidazole) has been immobilized on chloromethylated polystyrene (PS-Cl) cross-linked with divinylbenzene to obtain [V^VO_2(sal-aebmz)]@PS (**2**), a heterogeneous complex. Both complexes, after characterization, have been used as catalysts to explore a single pot multicomponent (benzaldehyde or its derivatives, urea and ethyl acetoacetate) Biginelli reaction producing biologically active 3,4-dihydropyrimidin-2-(1*H*)-one (DHPM)-based biomolecules under solvent-free conditions in the presence of H_2O_2 as a green oxidant. Various reaction conditions such as amounts of catalyst and oxidant, temperature, time, and solvent have been optimized to obtain the maximum yield of DHPMs. The polymer-immobilized complex has been found to show excellent catalytic activity, giving *ca*. 95% yield of DHPMs under the optimized reaction conditions selectively. Oxidant plays an important role in enhancing the yield of DHPMs.

Keywords: chloromethylated polystyrene; dioxidomolybdenum(VI) complex; multicomponent Biginelli reaction; solventless conditions; supported and unsupported catalysts

Citation: Maurya, M.R.; Patter, A.; Singh, D.; Ghosh, K. Polymer-Supported Dioxidovanadium(V) Complex-Based Heterogeneous Catalyst for Multicomponent Biginelli Reaction Producing Biologically Active 3,4-Dihydropyrimidin-2-(1*H*)-ones. *Catalysts* **2023**, *13*, 234. https://doi.org/10.3390/catal13020234

Academic Editor: Giovanna Bosica

Received: 3 December 2022
Revised: 11 January 2023
Accepted: 16 January 2023
Published: 19 January 2023

1. Introduction

In recent times, multicomponent reactions have been considered the green reaction and most efficient tools in modern synthetic organic chemistry [1] because (i) such reaction is able to produce a complex product using simple starting materials without producing any chemical waste, and (ii) generally, the product produced can simply be purified by crystallization process [2]. 3,4-Dihydropyrimidin-2-(1*H*)-one (DHPM) and its derivatives, generally synthesized through multicomponent Biginelli reaction [3–6], are known for their biological activities [7], such as antitumor, antiproliferative [8], anti-inflammatory [9,10], antimalarial [11], antitubercular [12], antidiabetic [13], antiepileptic [14], antileishmanial [15], anti-HIV [16], the intervention of human TLR4 (toll-like receptor 4) [17], etc. Even the thione analog dihydropyrimidine-2-thione is also known as a potential antitumor agent [18].

Different types of homogeneous and heterogeneous catalysts have been used for the synthesis of 3,4-dihydropyrimidin-2-(1*H*)-ones [5,19–34], but so far, the literature presents only limited reports on the use of metal complexes based on heterogeneous catalysts and that too from our research group [35]. Heterogeneous catalysts, particularly homogeneous complex-based catalysts immobilized on a solid support such as chloromethylated polystyrene cross-linked with divinylbenzene, have added advantages due to ease in their syntheses, their long life, easy recovery from the reaction mixture, and reusability [36]. Further, such polymeric (support) materials are commercially available in bulk at a low price and thus make heterogeneous catalysts relatively less expensive. With our continued interest in developing vanadium-based heterogeneous catalysts, we have now prepared a polymer-supported vanadium complex [V^VO_2(sal-aebmz)]@PS (where PS = chloromethylated polystyrene cross-linked with divinylbenzene, Hsal-aebmz = Schiff base derived from 2-aminoethylbenzimidazole and salicylaldehyde). Considering the green approach, the catalytic potential of this catalyst has been reported for the synthesis of various derivatives of 3,4-dihydropyrimidin-2-(1*H*)-one via multicomponent Biginelli reaction under solvent-free conditions in the presence of green oxidant H_2O_2. Catalytic formation of the corresponding thione derivatives, 3,4-dihydropyrimidine-2-(1*H*)-thiones, has also been tested.

2. Results and Discussion

2.1. Synthesis and Characterization of Heterogeneous Complex

Ligand Hsal-aebmz (**I**) reacts easily with aerially oxidized [$V^{IV}O(acac)_2$] [37] in refluxing methanol to provide [V^VO_2(sal-aebmz)] (**1**) [38]. Characterization details presented in the Experimental section (also see Figures S1 and S2) confirm its structure, and also spectral data compare well with the literature data [38]. Even complex **1** displays only one signal at –541.9 ppm in its ^{51}V NMR spectrum due to the presence of single species in the solution. Complex **1** can be anchored on chloromethylated polystyrene cross-linked with divinylbenzene (PS-Cl) to obtain catalyst [VO_2(sal-aebmz)]@PS (**2**) directly by reacting from its appended chloro group with the nitrogen of the imidazole group of complex **1** in DMF in slightly basic medium. The whole synthetic procedure is presented in Scheme 1. This heterogeneous catalyst **2** was characterized by thermal study, spectroscopic (FT-IR and UV-visible) studies, microwave plasma atomic emission spectroscopy (MP-AES), field emission-scanning electron microscopy (FE-SEM), and energy-dispersive spectroscopy (EDS) analyses. Comparison of the spectroscopic study of complex **1** also helped in characterizing **2** to some extent.

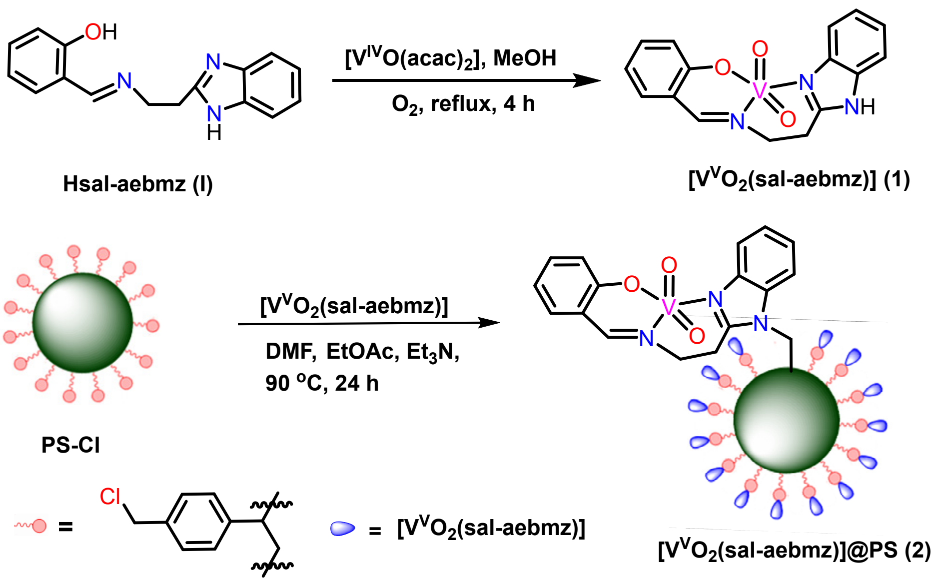

Scheme 1. Synthetic route to prepare [V^VO_2(sal-aebmz)]@PS (**2**).

2.2. Thermal Analysis

The homogeneous complex is stable up to ca. 200 °C. On further increasing the temperature, the ligand moiety of the complex starts decomposing and completes at 540 °C. The remaining mass represents V_2O_5 (obs.: 26.4%, Calc.: 26.2%) as the end product. The heterogeneous catalyst **2** is stable up to ca. 170 °C (Figure 1), and thereafter, it decomposes in three overlapping steps. From the TGA profile, it is clear that part of the ligand decomposed first as 12.8% mass loss was observed at ca. 265 °C. Immediately, the second step of decomposition started, which overlapped with the third step. Here, the remaining ligand's fragment and polymer backbone both decomposed with a total mass loss of 87.3% at 360 °C. At this temperature, decomposition stabilized to provide V_2O_5 equivalent to 12.7%.

The vanadium content calculated from the V_2O_5 residue was found to be 1.39 mmol/g of polymer, which is in suitable agreement with the result obtained by MP-AES (1.43 mmol/g).

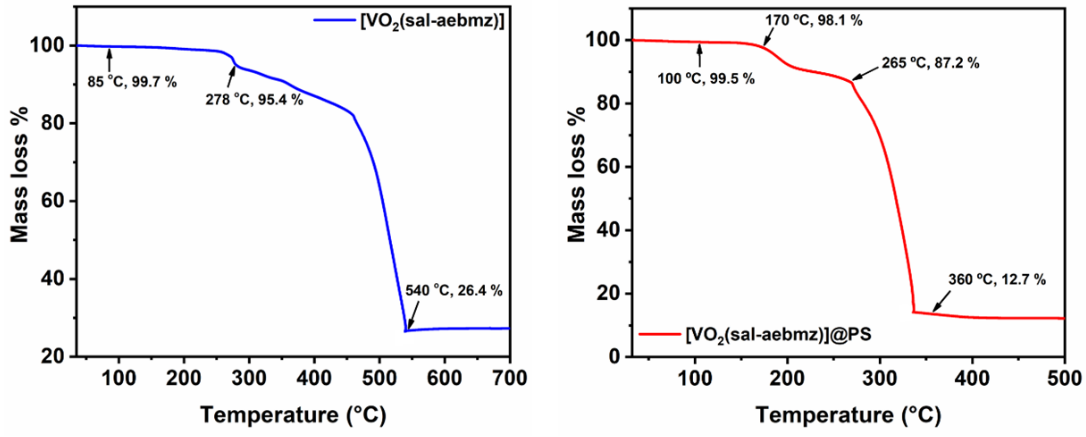

Figure 1. TGA profiles of [V^VO_2(sal-aebmz)] (**1**) and heterogeneous catalyst [V^VO_2(sal-aebmz)]@PS (**2**).

2.3. FT-IR Study

Figure 2 compares the FT-IR spectra of ligand and homogeneous complex **1** with heterogeneous catalyst **2**. Ligand **I** exhibits a sharp band at 1636 cm^{-1} due to ν(C=N) stretch, which shifts to a lower wavenumber and appears at 1625 cm^{-1} in complex **1** due to the coordination of azomethine/ring nitrogen to vanadium. The presence of a few weak intensity bands covering 2600–2900 cm^{-1} region in ligands as well as in complexes is due to CH_2/NH groups. In addition, **1** shows two sharp bands at 917 and 949 cm^{-1} arising due to *cis*-[VO_2] structure [38]. The intensity of most bands is weak/medium in the heterogeneous catalyst **2;** however, the band due to ν(C=N) stretch can be seen at 1631 cm^{-1}, which has been merged with ν(C=C) present in the polymer backbone. Only two/three medium-intensity bands have also been observed at ca. 2900 cm^{-1}, suggesting the presence of only the methylene group and the absence of the –NH group. The absence of band(s) due to the –NH group is due to its involvement in covalent bond formation with a polymer backbone. In addition, two weak bands at 948 and 919 cm^{-1} are indicative of the retention of *cis*-[VO_2] structure of complex **1** in heterogeneous catalyst **2**. The signal due to C-Cl is still present in the heterogeneous complex at 692 cm^{-1}, indicating that not all the Cl has been replaced by **1**.

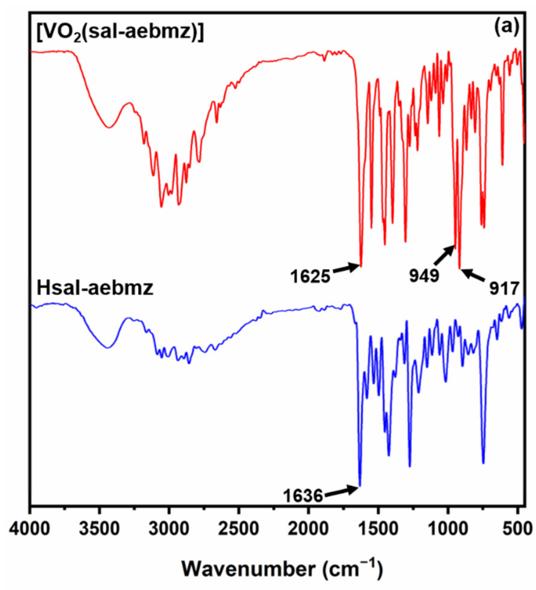

Figure 2. *Cont.*

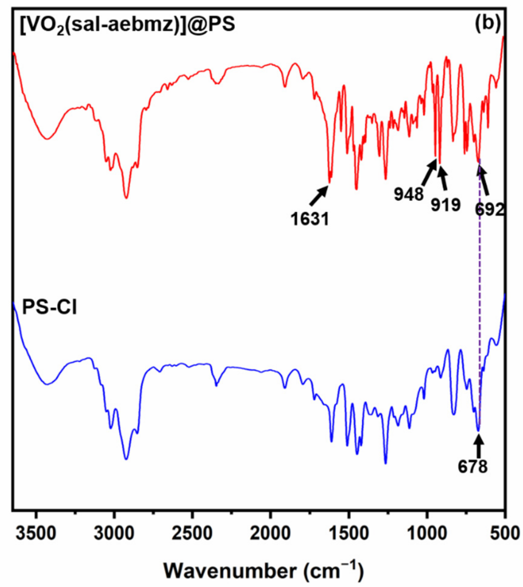

Figure 2. (**a**) FT-IR spectra of ligand Hsal-aebmz (**I**) and $[V^VO_2$(sal-aebmz)] (**1**). (**b**) FT-IR spectra of PS-Cl and heterogeneous catalyst $[V^VO_2$(sal-aebmz)]@PS (**2**).

2.4. UV-Visible Spectral Study

Figure 3a presents UV-visible spectra of ligand Hsal-aebmz and homogeneous complex $[V^VO_2$(sal-aebmz)] (**1**), and Figure 3b displays UV-visible spectra of PS-Cl and heterogeneous catalyst **2**. The UV region spectrum of ligands shows five intra-ligand bands at 207, 252, 273, 280, and 316 nm. Most of these bands also appear in complex **1,** but only two bands centered at 225 and 278 nm can be seen in catalyst **2**. Further, a weak shoulder band is located at 417 nm in **2,** while a band at 409 nm in **1** can be assigned due to ligand to metal charger transfer band. As expected, no such UV-visible bands are present in PS-Cl except one very weak shoulder at ca. 225 nm, which is possibly due to the aromatic ring present in polystyrene.

2.5. Field Emission-Scanning Electron Microscopy (FE-SEM) and Energy-Dispersive X-ray Analyses (EDS)

FE-SEM analysis was carried out to observe the morphological changes that occurred before and after the coordination of polystyrene beads. Images of fresh, polymer-supported beads, and polymer-supported beads after the first catalytic cycle, along with elemental mapping, are shown in Figure 4[(a-i)–(a-iv),(b-i)–(b-vi)]. The high-resolution images show slight smoothening of the surface of polymeric beads after the immobilization of the complex. Elemental mapping confirms the uniform attachment of the complex on the polymeric beads. However, energy-dispersive X-ray analysis shows the presence of a small amount of chlorine content even after complexation in the polymer, which suggests that not all the chlorine sites have been replaced by the complex. The energy-dispersive X-ray analysis of the polymer-supported complex estimates the vanadium content of 8.05 wt%, which confirms the successful immobilization of the vanadium complex onto chloromethylated polystyrene. FE-SEM analysis of recycled polymeric beads (see Figure 4[(c-i)–(c-vi)] and Figure S3) still shows the presence of V on the surface, but EDS analysis indicates slightly lower metal content (7.47 wt% for the first cycle vs. 8.05% for fresh sample) (Table S1) compared to the fresh catalyst, indicating that there is slight leaching of the metal complex during the catalytic reaction.

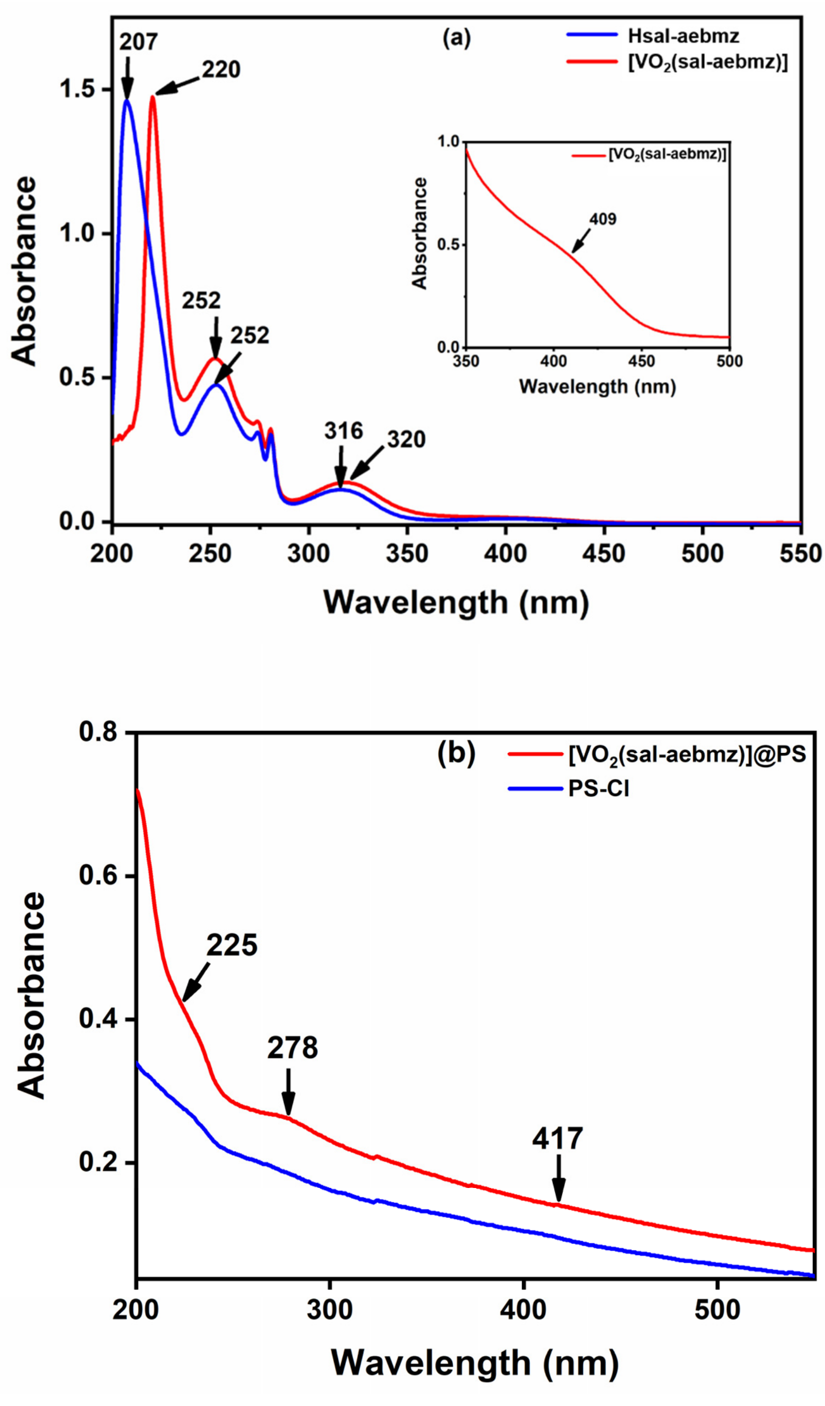

Figure 3. (**a**) UV-visible spectra of ligand Hsal-aebmz (**I**) and homogeneous complex $[V^VO_2$(sal-aebmz)] (**1**) recorded in MeOH. Inset shows a weak LMCT band of complex taken at higher concentration. (**b**) UV-visible spectra of PS-Cl and heterogeneous catalyst $[VO_2$(sal-aebmz)]@PS (**2**) recorded in Nujol.

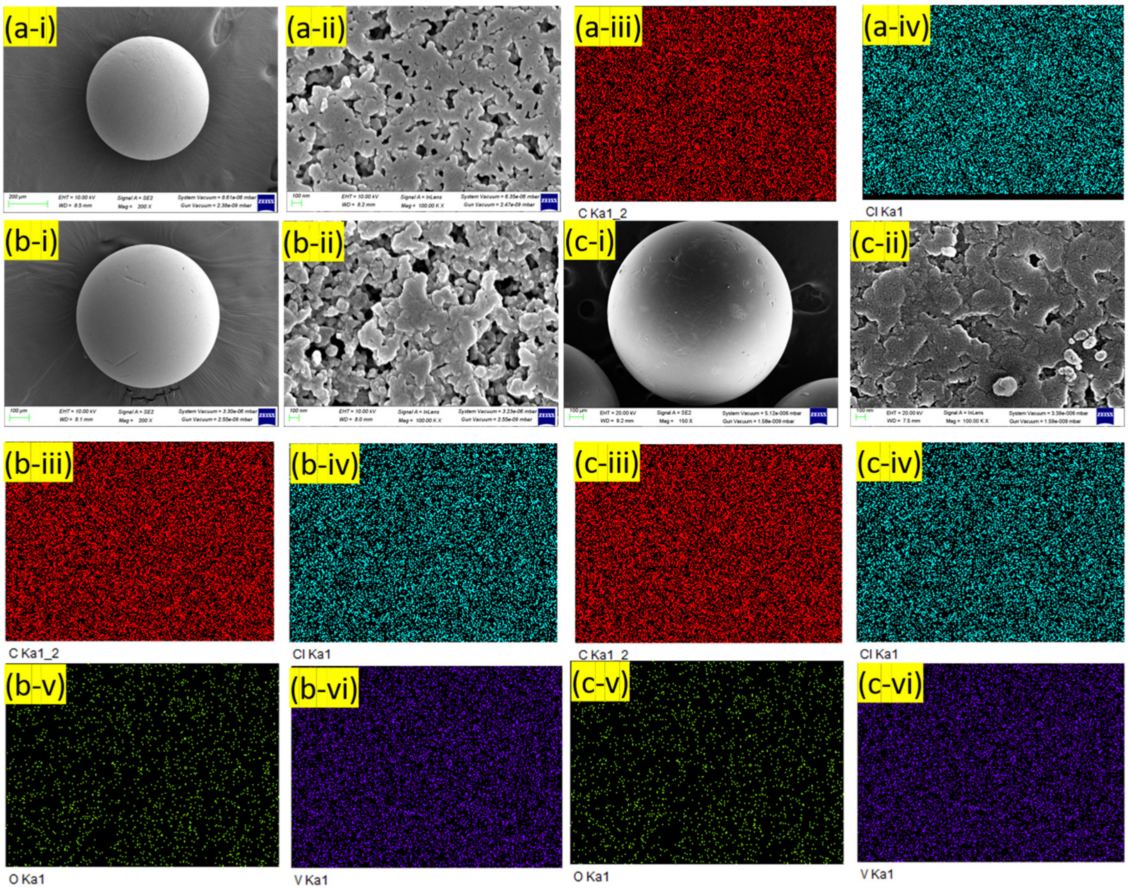

Figure 4. FE-SEM image (**a-i**), high-resolution FE-SEM image (**a-ii**), and elemental mapping of C (**a-iii**), and Cl (**a-iv**) of chloromethylated polystyrene (PS-Cl). FE-SEM image (**b-i**), high-resolution FE-SEM image (**b-ii**), elemental mapping of C (**b-iii**), Cl (**b-iv**), O (**b-v**) and V (**b-vi**) of [V^VO_2(sal-aebmz)]@PS. FE-SEM image (**c-i**), high-resolution FE-SEM image (**c-ii**), and elemental mapping of C (**c-iii**), Cl (**c-iv**), O (**c-v**), and V (**c-vi**) of [V^VO_2(sal-aebmz)]@PS after the first cycle.

2.6. Catalytic Activity Study-Multicomponent Biginelli Reaction for the Synthesis of 3,4-Dihydropyrimidin-2(1H)-ones

The multicomponent Biginelli reaction comprising of reactants benzaldehyde, ethyl acetoacetate and urea using a greener oxidant 30% aqueous H_2O_2 was carried out under solvent-free conditions using heterogeneous catalyst **2**. This resulted in the formation of the corresponding 3,4-dihydropyrimidin-2(1*H*)-one (DHPM) (Scheme 2) selectively.

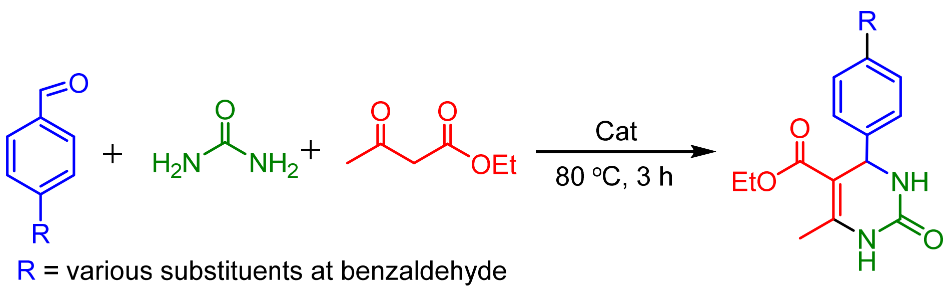

Scheme 2. Scheme for multicomponent Biginelli reaction for the synthesis of 3,4-dihydropyrimidin-2(1*H*)-one (DHPM).

Initially, the effect of solvents on this reaction was studied by considering multicomponent reagents (i.e., benzaldehyde (0.530 g, 5 mmol), ethyl acetoacetate (0.650 g, 5 mmol) and urea (0.360 g, 6 mmol)) in the presence of 0.015 g of catalyst **2** and H_2O_2 (1.13 g, 10 mmol).

After carrying out the reaction at 80 °C or at reflux temperature where the solvent boils below 80 °C for 3 h, the obtained results for the respective solvent, as well as under solvent-free conditions, are presented in Table 1. It is clear that a solvent-free reaction provides a much better result than carrying out a reaction in any polar or non-polar solvent.

Table 1. Screening of multicomponent Biginelli reaction under different solvent as well as solvent-free conditions.

S. No.	Solvent	Catalyst 2 (g)	H_2O_2 (g, mol)	Temp. (°C)	Isolated Yield (%)
1	CH_2Cl_2	0.015	1.13, 10	Reflux	15
2	CCl_4	0.015	1.13, 10	Reflux	14
3	MeCN	0.015	1.13, 10	80	12
4	Toluene	0.015	1.13, 10	80	18
5	MeOH	0.015	1.13, 10	Reflux	20
6	EtOH	0.015	1.13, 10	Reflux	18
7	Chloroform	0.015	1.13, 10	Reflux	5
8	Dioxane	0.015	1.13, 10	80	33
9	Solvent-free	0.015	1.13, 10	80	85

As mentioned in the Experimental section, rest reaction optimization was performed considering four different amounts of catalyst **2** (0.005, 0.010, 0.015, and 0.020 g) and three different amounts of 30% aqueous H_2O_2 (10, 15, and 20 mmol) while the reaction was carried out without using any solvent at ambient temperature, 70, 80, and 90 °C for 3 h. The amounts of multicomponent reagents were the same as mentioned above. Details of the reaction conditions and isolated yield of DHPM under a particular set of conditions are presented in Table 2. Figure 5 provides time vs. % yield for different reaction conditions. From these experiments it is clear that the best-suited reaction conditions are as presented in entry 6 of Table 2. Under these conditions, a maximum of 95% yield of DHPM was obtained. It is to be noted that blank reactions (either in the absence of catalyst or oxidant or none of these) provided much lower yields (entries 10–12 of Table 2).

Table 2. Details for multicomponent Biginelli reaction [multicomponent reagents: benzaldehyde (0.530 g, 5 mmol), ethyl acetoacetate (0.650 g, 5 mmol), and urea (0.36 g, 6 mmol)] to optimize the reaction condition for catalyst **2** under solvent-free conditions. Results were noted after 3 h of reaction.

S. No.	Catalyst (g)	H_2O_2 (g, mol)	Temp. (°C)	Isolated Yield (%)
1	0.005	1.13, 10	80	60
2	0.010	1.13, 10	80	75
3	0.015	1.13, 10	80	85
4	0.020	1.13, 10	80	89
5	0.015	1.69, 15	80	88
6 [a]	0.015	2.26, 20	80	95
9	0.015	1.13, 10	RT	15
7	0.015	1.13, 10	70	72
8	0.015	1.13, 10	90	91
10	-	1.13, 10	80	49
11	0.015	-	80	38
12	-	-	80	7

[a] Optimized reaction conditions.

2.7. Scope of the Biginelli Reaction to Other 3,4-Dihydropyrimidin-2 (1H)-ones

After observing suitable conversion by catalyst **2**, other aromatic mono aldehydes such as *p*–methylbenzaldehyde, *p*–methoxybenz aldehyde, *p*–bromobenzaldehyde, *p*–chlorobenzaldehyde, and *p*–nitrobenzaldehyde as well as bis(aldehyde) such as terepthaldehyde and other esters such as ethyl benzoyl acetate were also considered and yield of the corresponding DHPM for this model reaction was checked. Thus, under the optimized reaction conditions (entry 6 of Table 2), these multicomponent reagents in the presence of urea (same mmol of these as mentioned above) provided extremely suitable yields. Table 3 presents these details. All these products are isolable from the reaction mixture, which can also be crystallized from MeOH, though yield in the case of crystallization was found to be a little less (ca. 5%) than those obtained through column purification. These products were finally characterized by ^{1}H NMR and ^{13}C NMR spectroscopy (Table S2 and Figures S4–S21).

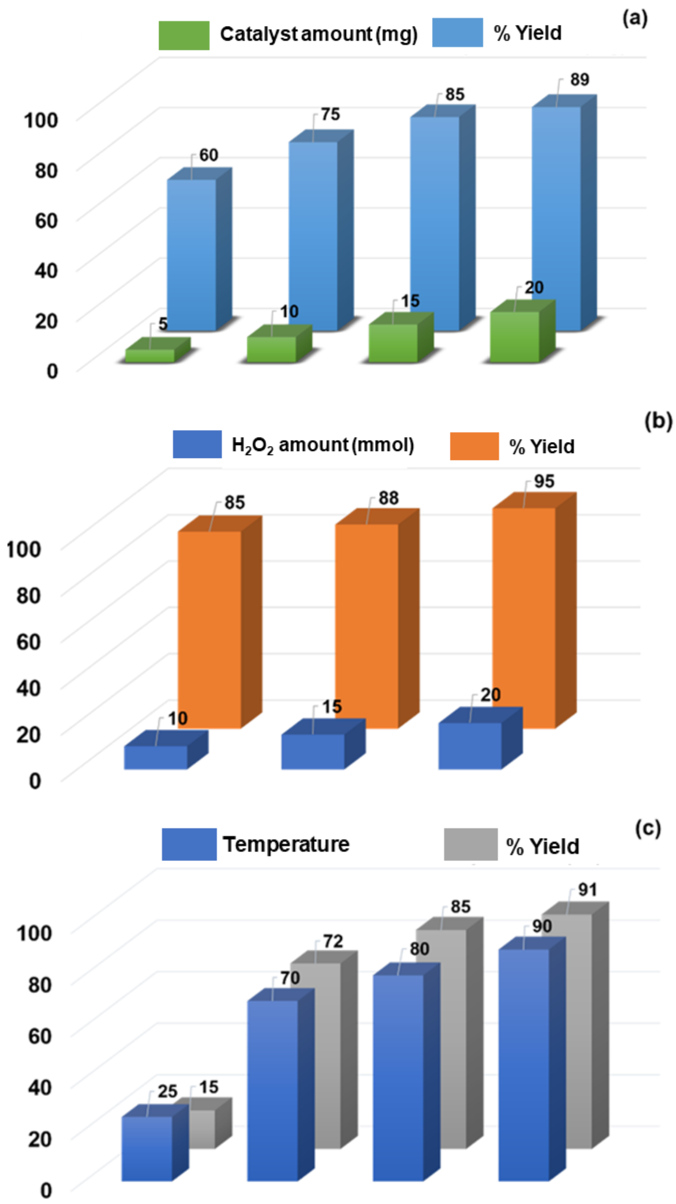

Figure 5. (**a**) Effect of different amounts of catalyst **2** (0.005, 0.010, and 0.015 g) on the yield using 30% aqueous H_2O_2 (1.13, 0.010 mol) at 80 °C. (**b**) Effect of different amounts of oxidant, i.e., 30% aqueous H_2O_2 (0.010, 0.015, and 0.020 mol), on the yield using catalyst **2** (0.0150 g) at 80 °C. (**c**) Effect of temperature variations (RT, 70, 80, and 90 °C) on the yield using catalyst **2** (0.0150 g) and 30% aqueous H_2O_2 (0.010 mol).

Table 3. Details for multicomponent Biginelli reaction for the synthesis of DHPM (reaction conditions: respective aldehyde (5 mmol), respective ester (5 mmol), urea (6 mmol), catalyst **2** (0.015 g), and aqueous 30% H_2O_2 (2.26, 20 mmol)) under solvent-free conditions at 80 °C for 3 h of reaction time.

S. No.	Aldehyde	Ester	Product	Isolated (After Crystallization) Yield (%)
1	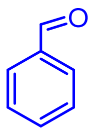	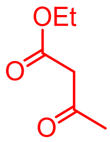	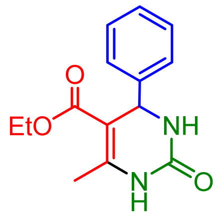	95 (91)
2	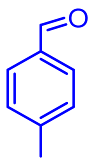	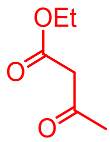	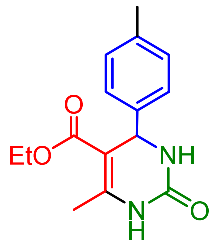	88 (82)
3	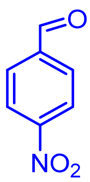	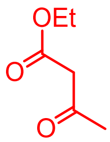	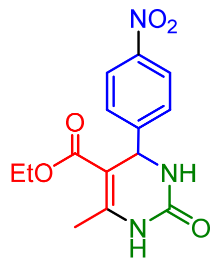	94 (90)
4	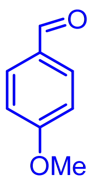	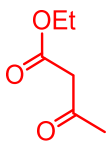	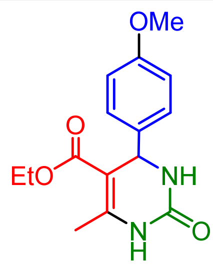	90 (86)
5	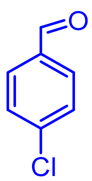	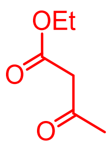	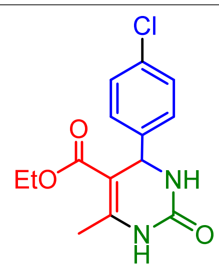	87 (82)
6	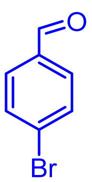	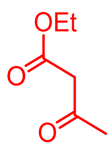	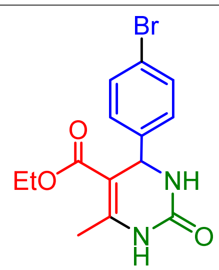	86 (84)

Table 3. *Cont.*

S. No.	Aldehyde	Ester	Product	Isolated (After Crystallization) Yield (%)
7	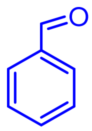	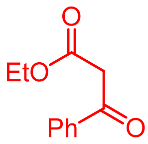	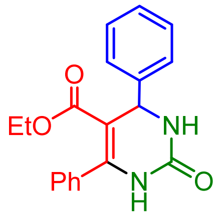	90 (85)
8	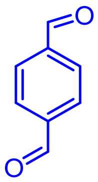	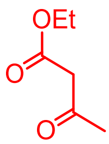	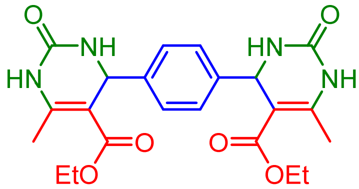	93 (88)
9	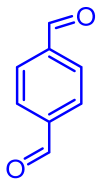	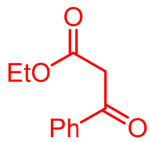	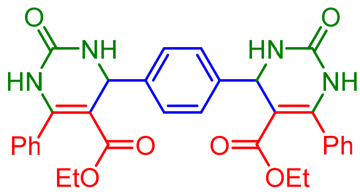	91 (86)

In order to further emphasize the catalytic utility of heterogeneous catalyst **2** for the synthesis of dihydropyrimidine-2-thione, a reaction of different aromatic aldehyde (5 mmol), ethyl acetoacetate (5 mmol), and thiourea (6 mmol) was carried out in the presence of catalyst **2** (0.015 g) under solvent-free conditions at 80 °C for 3 h. Since thiourea instantly reacts with H_2O_2, its use was avoided in these reactions. Table 4 presents the yield obtained (for ^{1}H and ^{13}C NMR of isolated compounds; see Table S3 and Figures S22–S33). It is clear that the catalyst is also active for the synthesis of dihydropyrimidine-2-thione, but the isolated yields are lower compared to the corresponding DHPMs isolated in the presence of H_2O_2. Thus, catalyst **2** works much better in the presence of oxidant H_2O_2.

2.8. Recyclability and Reusability Test

The recyclability details of the catalyst are presented in the Experimental section. Spectroscopic comparison (FT-IR and UV-visible studies) of the recycled and fresh catalyst **2** show similar spectral peaks (see Figures S34 and S35), suggesting the stability of the catalyst even after one use. Even FE-SEM analysis confirms no significant changes in the morphology of the recovered catalyst **2,** and elemental mapping by EDS (Figures 4 and S3) shows the presence of vanadium complex though the signal is slightly weaker than found in fresh catalyst [V content: 7.47 wt.% (recycled) vs. 8.05 wt.% (fresh catalyst)] (Table S1). This is possibly due to partial wash away of the loosely bound vanadium complex from the surface of polymer beads during catalytic reaction. However, the recycled catalyst exhibited equally suitable catalytic activity (Figure 6) for the synthesis of DHPMs under optimized reaction conditions for up to three catalytic cycles.

*2.9. Comparison of Catalytic Efficiency of Catalyst **2** with the Literature Data*

The catalytic efficiency of catalyst **2** compares well with the catalysts reported in the literature. Table 5 compares the yield of DHPM using various catalysts. It is clear that most catalysts have competing yields. However, catalysts at entries 1–5 require more time to complete the reaction, while metal complexes require relatively less time. Within supported vanadium complexes, the catalyst reported here and even earlier reported from our laboratory both are suitable and deliver an excellent yield of DHPMs under solvent-free reaction conditions.

Table 4. Details for multicomponent Biginelli reaction for the synthesis of dihydropyrimidine-2-thione (reaction conditions: respective aldehyde (5 mmol), ethyl acetoacetate (5 mmol), thiourea (6 mmol), and catalyst **2** (0.015 g)) under solvent-free conditions at 80 °C for 3 h of reaction time.

S. No.	Aldehyde	Ester	Amine	Product	Isolated Yield (%)
1	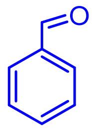	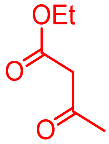	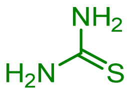	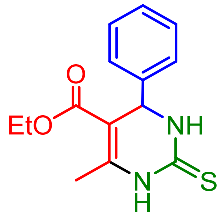	35
2	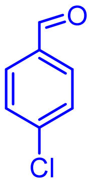	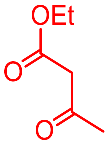	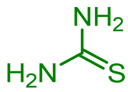	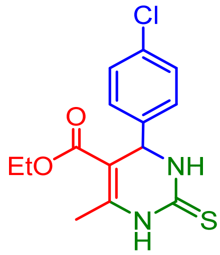	39
3	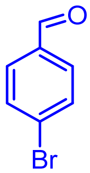	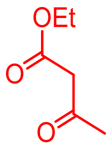	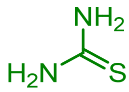	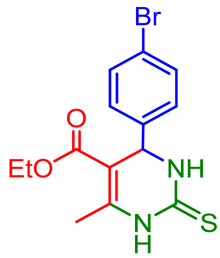	41
4	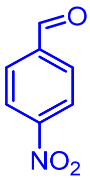	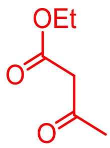	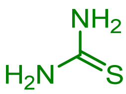	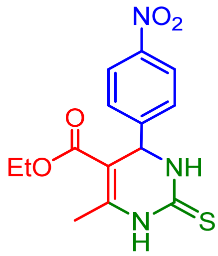	33
5	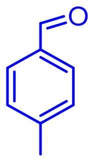	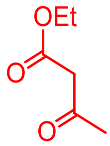	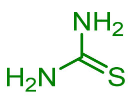	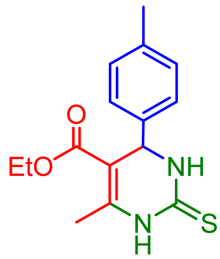	44
6	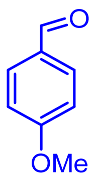	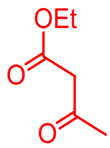	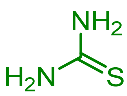	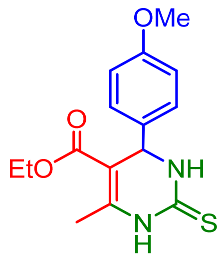	42

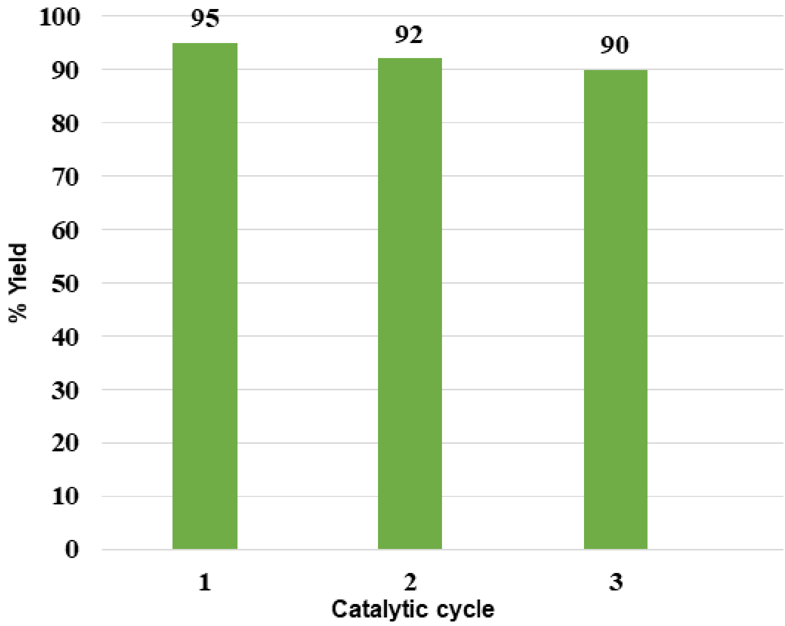

Figure 6. Recyclability details of catalyst **2**. Results of three cycles are shown.

Table 5. Comparison of the results of the synthesis of 3,4-dihydro-5-ethoxycarbonyl-4-(4-phenyl-6-methylpyrimidine-2(1*H*)-one using different catalysts.

Entry No.	Catalyst and Conditions	Reaction Time (h)	Yield (%)	Ref.
1	$BiCl_3$/MeCN/Δ	5	95	[39]
2	$FeCl_3.6H_2O$/EtOH/Δ	4	94	[40]
3	$CpTiCl_2$/EtOH/70 °C	9	99	[41]
4	MoO_2Cl_2	10	72	[42]
5 [a]	$[\{Mo^{VI}O_2(H_2O)\}_3L]$	3	95	[43]
6 [b]	PS–$[V^{V}O(OEt)(hptb)(EtOH)]$	1.5	91	[35]
7 [c]	$[\{V^{V}O\}en(3,5\text{-dtbb})_3]$/ solvent-free/80 °C	3	94	[44]
8	**1**/ solvent-free/80 °C	3	82	This work
9	**2**/ solvent-free/80 °C	3	94	This work

[a] H_6L = Schiff base derived from benzene-1,3,5-tricarbohydrazide and 3-acetyl-2-hydroxyl-6-methyl-4H-pyran-4-one. [b] H_3hptb = 4-[3,5-bis(2-hydroxyphenyl)-1,2,4-triazol-1-yl] benzoic acid. [c] $H_3en(3,5\text{–dtbb})_3$ = N,N-bis(2-hydroxy-3,5-ditertbutylbenzyl)-N′-2-hydroxy-3,5–ditertbutylbenzyledene-1,2-diaminoethane dianion.

2.10. Possible Reaction Mechanism

Since H_2O_2 influences the catalytic activity of the heterogeneous as well as homogeneous catalysts, it was important to propose a possible reaction mechanism. Therefore, a solution of complex $[V^{V}O_2(\text{sal-aebmz})]$ (1) was prepared in 10 mL of DMSO (2×10^{-4} M) and was titrated by adding one drop portion of 30% H_2O_2 dissolved in 10 mL of DMSO (final concentration of H_2O_2 solution: 9.5×10^{-2} M) and resulting spectral changes were monitored by UV-visible absorption spectrophotometer. The resulting changes are shown in Figure 7a. Thus, the intensity of bands appearing at 383, 276, and 258 nm shifts to the higher side without changing their positions while the intensity of the 313 nm band slightly goes down along with the generation of an isosbestic point at 310 nm (inset of Figure 7a). The generation of an isosbestic point hints toward the interaction of complex **1** with H_2O_2 and the generation of the corresponding peroxido complex. The ^{51}V NMR spectrum recorded in the presence of 40 equivalent of 30% aqueous H_2O_2 to a DMSO-d_6 solution of **1** also resulted in the generation of a new signal at –552.7 ppm in addition to the original signal at 541 ppm (Figure 8), which clearly approves the formation of peroxido complex in solution. In fact, the peroxido form of complex **1** has earlier been isolated and partially characterized [38]. Interaction of a solution of (a) with benzaldehyde causes a further increase in the intensities of bands at 383, 276, and 258 nm without changing the intensity as well as the position of the 313 nm band. At the same time, a new band at 293 nm also generates (Figure 7b). This clearly shows the interaction of the peroxido complex with benzaldehyde. The intensity of all bands undergoes a slight decrease in intensity upon the addition of urea (3×10^{-3} M) to a solution of (b) (Figure 7c). Similarly, the addition of one drop portion of ethyl acetoacetate (7.5×10^{-4} M) to a solution of (c) again causes only a slight decrease in the intensity of all bands. These observations suggest that urea and ethyl acetoacetate both interact with the complex but have less impact on metal centers. Based on the DFT study for oxidovanadium(V) complex for a similar multicomponent reaction [35] and the study presented here, it is reasonable to propose a mechanism as sketched in Scheme 3.

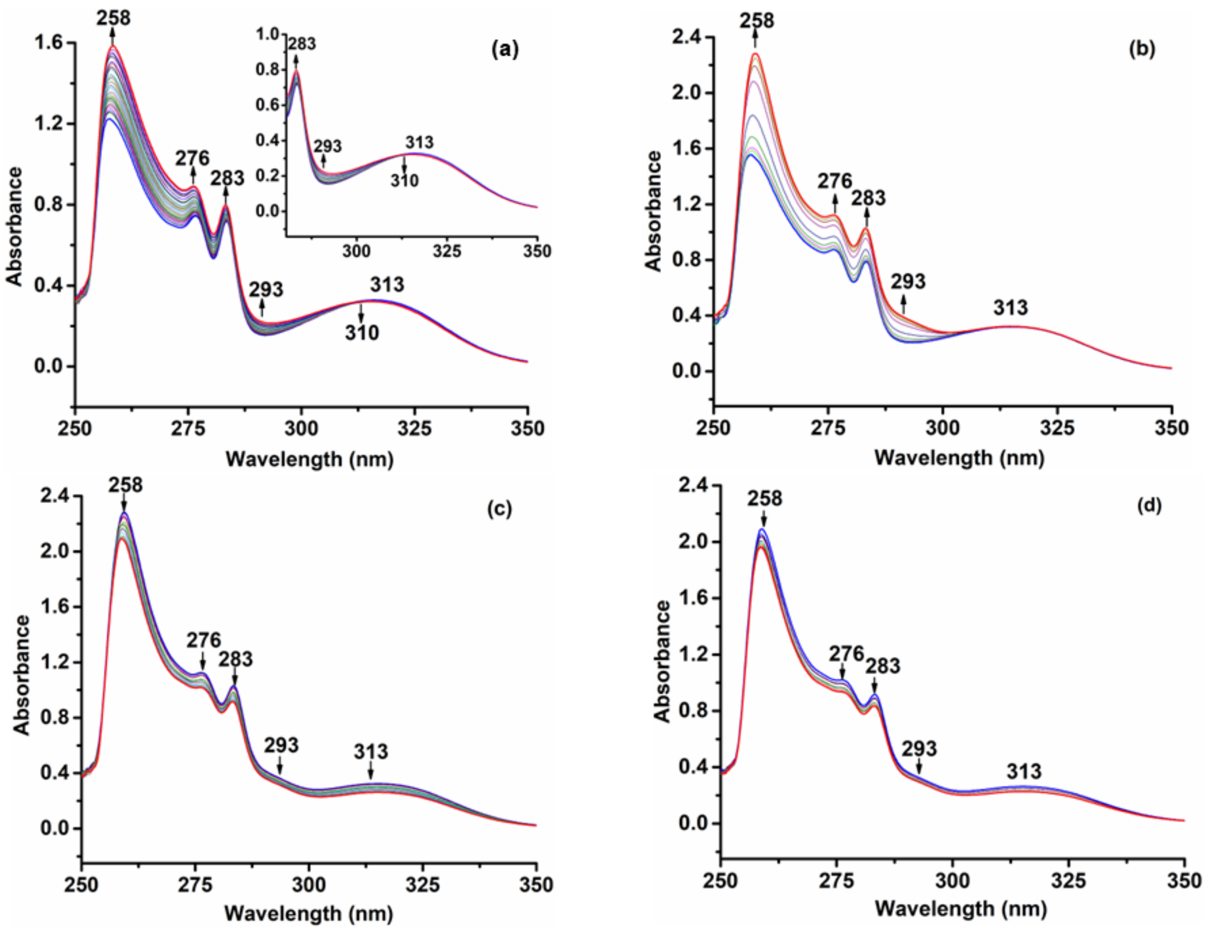

Figure 7. (**a**) Spectral changes observed after the successive addition of one drop portion of 30% H_2O_2 dissolved in 10 mL of DMSO (final concentration of H_2O_2 solution: 9.5×10^{-2} M) to 10 mL (2×10^{-4} M) solution of [V^VO_2(sal-aebmz)] (1) in DMSO. (**b**) Spectral changes observed after successive addition of one drop portion of benzaldehyde dissolved in 10 mL of DMSO (final concentration of benzaldehyde solution: 8×10^{-2} M) to a reaction mixture of (**a**). (**c**) Spectral changes observed after the successive addition of one drop portion of urea (3×10^{-3} M) to a solution of (**b**). (**d**) Spectral changes observed after the successive addition of one drop portion of ethyl acetoacetate (7.5×10^{-4} M) to a solution of (**c**).

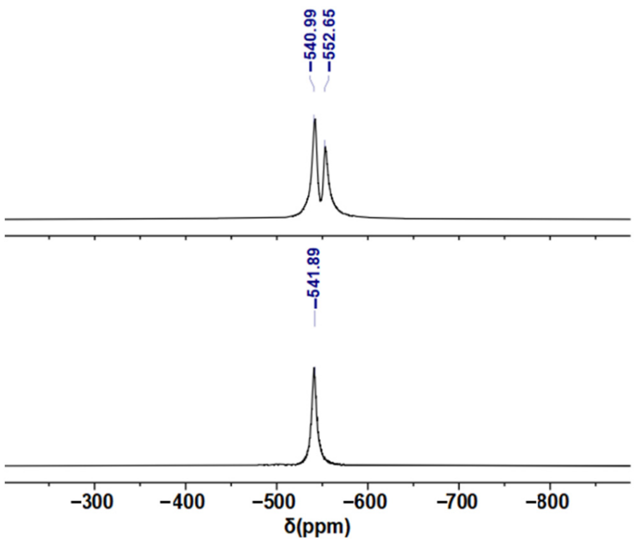

Figure 8. ^{51}V NMR spectrum of complex **1** in DMSO-d_6 (**bottom**) and after the addition of 40 equivalent of H_2O_2 to DMSO-d_6 solution of complex **1** (**top**).

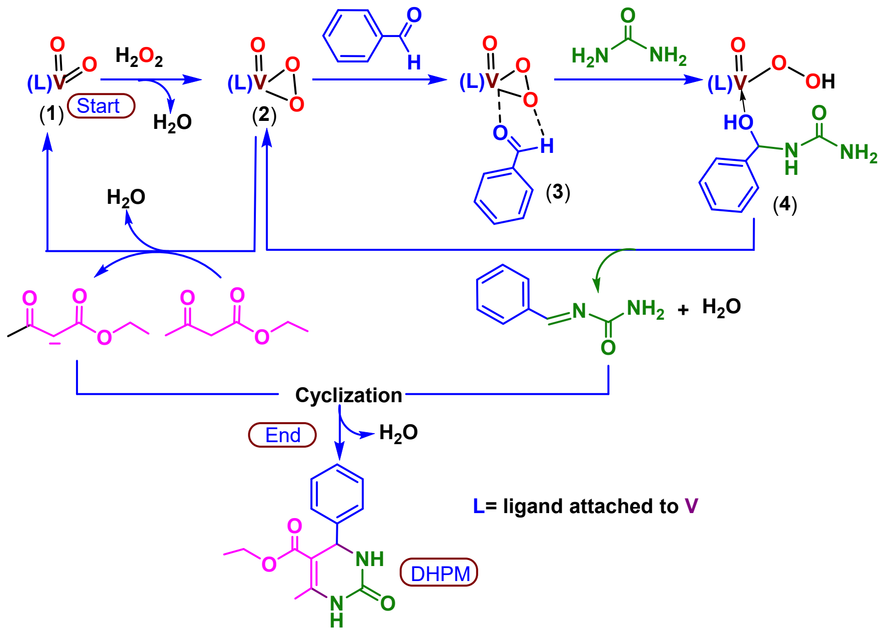

Scheme 3. Possible reaction mechanism for the three-component Biginelli reaction for the synthesis of 3,4-dihydropyrimidin-2-(1*H*)-one.

3. Experimental Section

3.1. Materials and Methods

Acetyl acetone, β-alanine, salicylaldehyde, *o*-phenylenediamine (Sisco Research Laboratories,, Mumbai, India), triethylamine (Sigma Aldrich, WI, USA), 30% aqueous H_2O_2 (Rankem, Delhi, India) were used as supplied. Benzaldehyde and its derivatives were used as received unless stated otherwise. Chloromethylated polystyrene (18.9% Cl (5.35 mmol Cl per gram of resin)) cross-linked with 5% divinylbenzene was obtained as a gift from Thermax Limited, Pune, India. Precursors, [$V^{IV}O(acac)_2$] [37], 2-aminoethylbenzimidazole dihydrochloride (aebmz·2HCl) [45] and Hsal-aebmz (**I**) [38] were synthesized by the methods reported in the literature.

3.2. Instrumentation and Characterization Procedure

Using KBr pellets, IR spectra of supported as well as unsupported compounds were recorded on a PerkinElmer FT-IR spectrometer. A Shimadzu UV-2600 UV-visible spectrophotometer was used to obtain spectra of ligand and homogeneous complex in MeOH, while titration of the complex with H_2O_2 was studied in DMSO. Spectra of the supported complex were obtained in Nujol. A Jeol 500 MHz spectrometer with a common parameter setting was applied to record ^{1}H and ^{13}C NMR of ligand **I** and complex **1** in DMSO-d_6. ^{51}V NMR spectrum of complex **1** was recorded using $VOCl_3$ as an internal standard. Thermogravimetric analysis was performed under an air atmosphere using an EXSTAR TG/DTA 6300 instrument. Vanadium content in the supported complex was determined by the MP-AES model Agilent Technologies 4210. A field emission-scanning electron microscope (FE-SEM) was used to study the surface morphology of the supported catalyst, and an attached energy-dispersive spectrometer (EDS) was used to obtain an elemental mapping. The sample was made conductive by coating a thin film of gold over it, which also protected it from surface charging and thermal damage by the electron beam. At the initial stage of the catalytic run, Shimadzu 2010 plus gas chromatograph fitted with an Rtx-1 capillary column (30 m × 0.25 mm × 0.25 μm) and a flame ionization detector were used to study the formation of the product.

*3.3. Synthesis of [V^VO_2(sal-aebmz)] (**1**)*

A slight modification was made in the literature-reported method to synthesize **1** [38]. A solution of [V^{IV}O(acac)$_2$] (1.33 g, 5 mmol) in 50 mL methanol [38], after overnight aerial oxidation, was added to a methanolic solution (10 mL) of Hsal-aebmz (1.33 g, 5 mmol) and the reaction mixture was refluxed for 4 h on a water bath. After reducing the solvent volume to ca. 25 mL and cooling the reaction mixture to room temperature, the yellow solid precipitated out. The solid was filtered, washed with cold methanol, and dried in vacuum. Yield 0.950 g (57%). Selected IR data (KBr, $\overline{\nu}$/cm^{-1}): 1625 (C=N azomethine/N ring), 949, 917 (cis–[VO_2]). UV-Vis (MeOH) (λ_{max}/nm (ε, liter mol^{-1} cm^{-1})): 258 (11340), 276 (6980), 283 (6460), 313 (2740), 405(300). ^{1}H NMR (DMSO-d_6, δ/ppm): 13.37 (br, 1H, NH), 8.93 (d, *J* = 8.0 Hz, 1H, aromatic), 8.87 (s, 1H, -CH=N-), 7.55 (dd, J = 15.7, 7.8 Hz, 2H, aromatic), 7.39 (m, 3H, aromatic), 6.80 (dd, J = 14.0, 6.5 Hz, 2H, aromatic), 4.18 (t, J = 5.8 Hz, 2H, -N-CH_2-), 3.41 (t, J = 5.8 Hz, 2H, Ar-CH_2-). ^{13}C NMR (DMSO-d_6, δ/ppm): 172.26, 169.87, 164.02, 156.30, 144.78, 137.15, 135.78, 135.11, 126.21, 124.69, 121.96, 119.91, 114.78, 59.83, 33.66. ^{51}V NMR (DMSO-d_6, δ/ppm): −541.9. In the presence of H_2O_2: −541.0 and −552.7.

*3.4. Synthesis of [V^VO_2(sal-aebmz)]@PS (**2**)*

Chloromethylated polystyrene (1.5 g) was allowed to swell in DMF (12 mL) in a 100 mL round bottom flask for 2 h. A solution of [V^VO_2(sal-aebmz)] (0.700 g, 2 mmol) dissolved in DMF (12 mL) was added to the above suspension along with triethylamine (2.66 g, 26 mmol) and ethyl acetate (10 mL). The reaction mixture was continuously stirred for 24 h at 90 °C. After this, the reaction mixture was cooled down, filtered, washed with hot DMF (4 × 5 mL) followed by methanol (2 × 5 mL), and dried in an oven overnight at 120 °C to obtain gray-colored resin. The vanadium content found by MP-AES is 1.43 mmol/g.

3.5. Catalytic Activity Study: A Multicomponent Biginelli Reaction for the Synthesis of 3,4-Dihydropyrimidin-2(1H)-ones (DHPMs)

For the multicomponent synthesis of 3,4-dihydropyrimidin-2(1*H*)-one, the Biginelli reagents, benzaldehyde (0.530 g, 5 mmol), ethyl acetoacetate (0.650 g, 5 mmol) and urea (0.360 g, 6 mmol) were initially taken, and after addition of catalysts **2** (0.015 g) and 30% H_2O_2 (2.26 g, 0.020 mol), the reaction mixture was heated at 80 °C in an oil bath for 3 h along with slow stirring. Progress of the reaction was tracked by taking out a small portion of the reaction mixture at a set time interval. This reaction mixture was extracted with n-hexane and analyzed by gas chromatography. After completing the reaction, i.e., after ca. 3 h, the solid mixture was extracted with ethyl acetate (3 × 30 mL) and washed with a brine solution. The separated organic layer was dried over anhydrous Na_2SO_4 and evaporated to dryness to obtain a solid product. This was finally recrystallized with MeOH to obtain pure DHPM.

Amounts of catalyst and oxidant were varied, and their effect on the isolated yield of the product was analyzed at different reaction temperatures for the most suitable reaction conditions. The reaction was also carried out in the absence of an oxidant to study its influence on the yield. Other Biginelli reagents, such as other aromatic aldehydes and keto-esters, were varied to study the scope of the reaction.

3.6. Catalyst Recyclability Experiment

Once the reaction was complete, the heterogeneous catalyst was separated by simple filtration and washed with ethyl acetate and methanol. From such two efforts, the recovered catalyst [V^VO_2(sal-aebmz)]@PS was then dried in an air oven at 100 °C overnight and used for the next cycle. The procedure for the recycled catalyst is the same as that of the fresh catalyst used in the multicomponent Biginelli reaction.

4. Conclusions

Heterogeneous catalyst [V^VO_2(sal-aebmz)]@PS (**2**) has been developed by immobilizing dioxidovanadium(V) complex [V^VO_2(sal-aebmz)] (**1**) on chloromethylated polystyrene cross-linked with divinylbenzene and used as a catalyst for a single pot multicomponent (benzaldehyde or its derivatives, urea, and ethyl acetoacetate) Biginelli reaction. The reaction was very successful for producing biologically active 3,4-dihydropyrimidine (DHPM)-based biomolecules under solvent-free conditions in the presence of H_2O_2 as a green oxidant. Use of oxidant H_2O_2 has been found to be essential to enhance the yield of DHPMs. During the catalytic reaction, the vanadium complex reacts with H_2O_2 to provide the corresponding peroxidovanadium(V) complex, which reacts with aromatic aldehyde and facilitates multicomponent cycloaddition product [35]. This reaction is also extendable to various aromatic mono aldehydes such as *p*–methylbenzaldehyde, *p*–methoxybenzaldehyde, *p*–bromobenzaldehyde, *p*–chlorobenzaldehyde, and *p*–nitrobenzaldehyde as well as bis(aldehyde) such as tereptha-laldehyde and esters such as ethyl acetoacetate and ethyl benzoyl acetate, and in all cases, a suitable yield of the corresponding 3,4-dihydropyrimidine was obtained. Using thiourea in place of urea, the reaction also proceeds, but the overall yield of the corresponding dihydropyrimidine-2-thione is poor compared to DHPMs obtained in the presence of H_2O_2. Catalyst **2** is recyclable and reusable with minimum loss in its catalytic activity.

Supplementary Materials: The following supporting information can be downloaded at: https://www.mdpi.com/article/10.3390/catal13020234/s1, Figure S1: ^{1}H NMR spectra of Hsal-aebmz (**I**) and complex [V^VO_2(sal-aebmz)] (**1**); Figure S2: ^{13}C NMR spectra of Hsal-aebmz (**I**) and complex [V^VO_2(sal-aebmz)] (**1**); Figure S3: EDX analysis of fresh catalyst **2** (a) and after first catalytic cycle of **2** (b); Figure S4: ^{1}H NMR spectrum of 5-pyrimidinecarboxylic acid, 1,2,3,4-tetrahydro-6-methyl-2-oxo-4-phenyl-, ethyl ester; Figure S5: ^{13}C NMR spectrum of 5-pyrimidinecarboxylic acid, 1,2,3,4-tetrahydro-6-methyl-2-oxo-4-phenyl-, ethyl ester; Figure S6: ^{1}H NMR spectrum of 5-pyrimidinecarboxylic acid, 1,2,3,4-tetrahydro-4-(4-methylphenyl)-2-oxo-, ethyl ester; Figure S7: ^{13}C NMR spectrum of 5-pyrimidinecarboxylic acid, 1,2,3,4-tetrahydro-4-(4-methylphenyl)-2-oxo-, ethyl ester; Figure S8: ^{1}H NMR spectrum of 5-pyrimidinecarboxylic acid, 1,2,3,4-tetrahydro-4-(4-nitrophenyl)-2-oxo-, ethyl ester; Figure S9: ^{13}C NMR spectrum of 5-pyrimidinecarboxylic acid, 1,2,3,4-tetrahydro-4-(4-nitrophenyl)-2-oxo-, ethyl ester; Figure S10: ^{1}H NMR spectrum of 5-pyrimidinecarboxylic acid, 1,2,3,4-tetrahydro-4-(4-methoxyphenyl)-2-oxo-, ethyl ester; Figure S11: ^{13}C NMR spectrum of 5-pyrimidinecarboxylic acid, 1,2,3,4-tetrahydro-4-(4-methoxyphenyl)-2-oxo-, ethyl ester; Figure S12: ^{1}H NMR spectrum of 5-pyrimidinecarboxylic acid, 1,2,3,4-tetrahydro-4-(4-chlorophenyl)-2-oxo-, ethyl ester; Figure S13: ^{13}C NMR spectrum of 5-pyrimidinecarboxylic acid, 1,2,3,4-tetrahydro-4-(4-chlorophenyl)-2-oxo-, ethyl ester; Figure S14: ^{1}H NMR spectrum of 5-pyrimidinecarboxylic acid, 1,2,3,4-tetrahydro-4-(4-bromophenyl)-2-oxo-, ethyl ester; Figure S15: ^{13}C NMR spectrum of 5-pyrimidinecarboxylic acid, 1,2,3,4-tetrahydro-4-(4-bromophenyl)-2-oxo-, ethyl ester; Figure S16: ^{1}H NMR spectrum of ethyl 2-oxo-4,6-diphenyl-1,2,3,4-tetrahydropyrimidine-5-

carboxylate; Figure S17: ^{13}C NMR spectrum of ethyl 2-oxo-4,6-diphenyl-1,2,3,4-tetrahydropyrimidine-5-carboxylate; Figure S18: ^{1}H NMR spectrum of 5-pyrimidinecarboxylic acid, 4,4′-(1,4-phenylene)bis [1,2,3,4-tetrah ydro-6-methyl-2-oxo-, 5,5′-diethyl ester; Figure S19: ^{13}C spectrum of 5-pyrimidinecarboxylic acid, 4,4′-(1,4-phenylene)bis[1,2,3,4-tetrahydro-6-methyl-2-oxo-, 5,5′-diethyl ester; Figure S20: ^{1}H NMR spectrum of 5-pyrimidinecarboxylic acid, 4,4′-(1,4-phenylene)bis[1,2,3,4-tetrahydro-6-phenyl-2-oxo-, 5,5′-diethyl ester; Figure S21: ^{13}C spectrum of 5-pyrimidinecarboxylic acid, 4,4′-(1,4-phenylene) bis[1,2,3,4-tetrahydro-6-phenyl-2-oxo-, 5,5′-diethyl ester; Figure S22: ^{1}H NMR spectrum of ethyl 6-methyl-4-phenyl-2-thioxo-1,2,3,4-tetrahydropyrimidine-5-carboxylate; Figure S23: ^{13}C NMR spectrum of ethyl 6-methyl-4-phenyl-2-thioxo-1,2,3,4-tetrahydropyrimidine-5-carboxylate; Figure S24: ^{1}H NMR spectrum of ethyl 4-(4-chlorophenyl)-6-methyl-2-thioxo-1,2,3,4-tetrahydropyrimidine-5-carboxylate; Figure S25: ^{13}C NMR spectrum of ethyl 4-(4-chlorophenyl)-6-methyl-2-thioxo-1,2,3,4-tetrahydropy rimidine-5-carboxylate; Figure S26: ^{1}H NMR spectrum of ethyl 4-(4-bromophenyl)-6-methyl-2-thioxo-1,2,3,4-tetrahydropyrimidine-5-carboxylate; Figure S27: ^{13}C NMR spectrum of ethyl 4-(4-bromophenyl)-6-methyl-2-thioxo-1,2,3,4-tetrahydropyrimidine-5-carboxylate; Figure S28: ^{1}H NMR spectrum of ethyl 4-(4-nitrophenyl)-6-methyl-2-thioxo-1,2,3,4-tetrahydropyrimidine-5-carboxylate; Figure S29: ^{13}C NMR spectrum of ethyl 4-(4-nitrophenyl)-6-methyl-2-thioxo-1,2,3,4-tetrahydropyri midine-5-carboxylate; Figure S30: ^{1}H NMR spectrum of ethyl 6-methyl-2-thioxo-4-(p-tolyl)-1,2,3,4-tetrahydrop yrimidine-5-carboxylate; Figure S31: ^{13}C NMR spectrum of ethyl 6-methyl-2-thioxo-4-(p-tolyl)-1,2,3,4-tetrahydropyrimidine-5-carboxylate; Figure S32: ^{1}H NMR spectrum of ethyl 4-(4-methoxyphenyl)-6-methyl-2-thioxo-1,2,3,4-tetrahydropyrimidine-5-carboxylate; Figure S33: ^{13}C NMR spectrum of ethyl 4-(4-methoxyphenyl)-6-methyl-2-thioxo-1,2,3,4-tetrahydropyrimidine-5-carboxylate; Figure S34: IR spectrum of catalyst **2** after first catalytic cycle; Figure S35: UV-visible spectrum of catalyst **2** recorded in Nujol after first cycle; Table S1: Elemental mapping data from EDX analysis for fresh and recycled catalyst; Table S2: ^{1}H and ^{13}C NMR of synthesized 3,4–dihydropyrimidin–2 (1*H*)–ones; Table S3: ^{1}H and ^{13}C NMR spectral data of some synthesized dihydropyrimidine-2-thione. References [46–50] are cited in the Supplementary Materials.

Author Contributions: Conceptualization, M.R.M.; methodology, A.P. and D.S.; software, M.R.M., A.P. and D.S.; formal analysis, A.P. and D.S.; investigation, A.P. and D.S.; writing—original draft preparation, A.P. and D.S.; writing—review and editing, M.R.M. and K.G.; visualization, A.P. and D.S.; supervision, M.R.M. and K.G. project administration, M.R.M.; funding acquisition, M.R.M. All authors have read and agreed to the published version of the manuscript.

Funding: This research was funded by the Science and Engineering Research Council (CRG/2018/000182), the Department of Science and Technology, New Delhi, the Government of India.

Data Availability Statement: The datasets generated during and/or analyzed during the current study are available from the corresponding author on request.

Acknowledgments: M.R.M. thanks the Science and Engineering Research Council, the Department of Science and Technology, the Government of India, New Delhi, for financial support of the work. A.P. is thankful to the Council of Scientific and Industrial Research, New Delhi, for Junior Research Fellowship. The 500 MHz NMR used for study was purchased from DST-FIST grant by the department.

Conflicts of Interest: There are no conflict to declare.

References

1. Wender, P.A. Toward the ideal synthesis and molecular function through synthesis- informed design. *Nat. Prod. Rep.* **2014**, *31*, 433–440. [CrossRef] [PubMed]
2. Bosica, G.; Abdilla, R. Recent Advances in Multicomponent Reactions Catalysed under Operationally Heterogeneous Conditions. *Catalysts* **2022**, *12*, 725. [CrossRef]
3. Kapp, C.O. Recent Advances in the Biginelli Dihydropyrimidine Synthesis. New Tricks from an Old Dog. *Acc. Chem. Res.* **2000**, *33*, 879–888. [CrossRef]
4. Lusch, M.J.; Tallarico, J.A. Demonstration of the feasibility of a direct solid phase split-pool Biginelli synthesis of 3, 4-dihydropyrimidinones. *Org. Lett.* **2004**, *6*, 3237–3240. [CrossRef]
5. Zheng, L.; Wang, Y.; Li, X.; Zhang, W. Deep eutectic solvent/benzenesulfonic acid: An environmental friendly catalyst system towards the synthesis of dihydropyrimidinones via Biginelli reaction. *Chin. J. Org. Chem.* **2022**, *42*, 3714–3720.
6. Roy, K.D.; Bordoloi, M. Synthesis of some substituted 2-oxo-1,2,3,4-tetrahydropyrimidines (3,4-dihydropyrimidin-2(1)-ones) and 2-thioxo-1,2,3,4-tetrahydropyrimidines, catalyzed by tin(II) chloride dihydrate and tin(II) iodide under microwave irradiation. *Indian J. Chem.* **2006**, *45*, 1067–1071. [CrossRef]

7. Wan, J.-P.; Pan, Y. Recent advance in the pharmacology of dihydropyrimidinone. *Mini Rev. Med. Chem.* **2012**, *12*, 337–349. [CrossRef]
8. Treptow, T.G.M.; Figueiro, F.; Jandrey, E.H.F.; Battastini, A.M.O.; Salbego, C.G.; Hoppe, J.B.; Taborda, P.S.; Rosa, S.B.; Piovesan, L.A.; Montes D'Oca, C.D.R.; et al. Novel hybrid DHPM-fatty acids: Synthesis and activity against glioma cell growth in vitro. *Eur. J. Med. Chem.* **2015**, *95*, 552–562. [CrossRef]
9. Tozkoparan, B.; Ertan, M.; Kelicen, P.; Demirdamar, R. Synthesis and antiinflammatory activities of some thiazolo [3, 2-a] pyrimidine derivatives. *IL Farm.* **1999**, *54*, 588–593. [CrossRef]
10. Bahekar, S.S.; Shinde, D.B. Synthesis and anti-inflammatory activity of some [4, 6- (4-substituted aryl)-2-thioxo-1, 2, 3, 4-tetrahydro-pyrimidin-5-yl]-acetic acid derivatives. *Bioorg. Med. Chem. Lett.* **2004**, *14*, 1733–1736. [CrossRef]
11. Singh, K.; Kaur, T. Pyrimidine-based antimalarials: Design strategies and antiplasmodial effects. *Med. Chem. Commun.* **2016**, *7*, 749–768. [CrossRef]
12. Chikhale, R.; Menghani, S.; Babu, R.; Bansode, R.; Bhargavi, G.; Karodia, N.; Rajasekharan, M.V.; Paradkar, A.; Khedekar, P. Development of selective DprE1 inhibitors: Design, synthesis, crystal structure and antitubercular activity of benzothiazolylpyrimidine-5-carboxamides. *Eur. J. Med. Chem.* **2015**, *96*, 30–46. [CrossRef] [PubMed]
13. Dhumaskar, K.L.; Meena, S.N.; Ghadi, S.C.; Tilve, S.G. Graphite catalyzed solvent free synthesis of dihydropyrimidin-2 (1H)-ones/thiones and their antidiabetic activity. *Bioorg. Med. Chem. Lett.* **2014**, *24*, 2897–2899. [CrossRef] [PubMed]
14. Lewis, R.W.; Mabry, J.; Polisar, J.G.; Eagen, K.P.; Ganem, B.; Hess, G.P. Dihydropyrimidinone positive modulation of δ-subunit-containing γ-aminobutyric acid type A receptor, including an epilepsy-linked mutant variant. *Biochemistry* **2010**, *49*, 4841–4851. [CrossRef]
15. Rashid, U.; Sultana, R.; Shaheen, N.; Hassan, S.F.; Yaqoob, F.; Ahmad, M.J.; Iftikhar, F.; Sultana, N.; Asghar, S.; Yasinzai, M.; et al. Structure based medicinal chemistry-driven strategy to design substituted dihydropyrimidines as potential antileishmanial agents. *Eur. J. Med. Chem.* **2016**, *115*, 230–244. [CrossRef]
16. Hua, H.M.; Peng, J.; Dunbar, D.C.; Schinazi, R.F.; Andrews, A.G.C.; Cuevas, C.; Garcia-Fernandez, L.F.; Kelly, M.; Hamann, M.T. Batzelladine alkaloids from the caribbean sponge Monanchora unguifera and the significant activities against HIV1 and AIDS opportunistic infectious pathogens. *Tetrahedron* **2007**, *63*, 11179–11188. [CrossRef]
17. Zhou, M.; Wang, Y.; Lin, X.; Wan, J.; Wen, C. Specific TLR4 blocking effect of a novel 3,4-dihydropyrimidinone derivative. *Front. Pharmcol.* **2021**, *11*, 624059. [CrossRef]
18. González-Hernández, E.; Aparicio, R.; Garayoa, M.; José Montero, M.; Sevilla, M.Á.; Pérez-Meler, C. Dihydropyrimidine-2-thiones as Eg5 inhibitors and L-type calcium channel blockers: Potential antitumour dual agents. *Med. Chem. Commun.* **2019**, *10*, 1589–1598. [CrossRef]
19. Chen, W.; Qin, S.; Jin, J. HBF4-catalyzed Biginelli reaction: One-pot synthesis of dihydropyrimidin-2 (1H)-ones under solvent-free conditions. *Catal. Commun.* **2007**, *8*, 123–126. [CrossRef]
20. Shen, Z.L.; Xu, X.P.; Ji, S.J. Brønsted base-catalyzed one-pot three-component Biginelli-type reaction: An efficient synthesis of 4, 5, 6-triaryl-3, 4- dihydropyrimidin-2 (1H)-one and mechanistic study. *J. Org. Chem.* **2010**, *75*, 1162–1167. [CrossRef]
21. Starcevich, J.T.; Laughlin, T.J.; Mohan, R.S. Iron(III) tosylate catalyzed synthesis of 3, 4-dihydropyrimidin-2 (1H)-ones/thiones via the Biginelli reaction. *Tetrahedron Lett.* **2013**, *54*, 983–985. [CrossRef]
22. Kolvari, E.; Koukabi, N.; Armandpour, O. A simple and efficient synthesis of 3, 4- dihydropyrimidin-2-(1H)-ones via Biginelli reaction catalyzed by nanomagneticsupported sulfonic acid. *Tetrahedron* **2014**, *70*, 1383–1386. [CrossRef]
23. Pramanik, M.; Bhaumik, A. Phosphonic acid functionalized ordered mesoporous material: A new and ecofriendly catalyst for one-pot multicomponent Biginelli reaction under solvent-free conditions. *ACS Appl. Mater. Interfaces* **2014**, *6*, 933–941. [CrossRef] [PubMed]
24. Mondal, J.; Sen, T.; Bhaumik, A. Fe_3O_4@mesoporous SBA-15: A robust and magnetically recoverable catalyst for one-pot synthesis of 3, 4-dihydropyrimidin-2 (1*H*)-ones via the Biginelli reaction. *Dalton Trans.* **2012**, *41*, 6173–6181. [CrossRef]
25. Tamaddon, F.; Moradi, S. Controllable selectivity in Biginelli and Hantzsch reactions using nanoZnO as a structure base catalyst. *J. Mol. Catal. A Chem.* **2013**, *370*, 117–122. [CrossRef]
26. Titova, Y.; Fedorova, O.; Rusinov, G.; Vigorov, A.; Krasnov, V.; Murashkevich, A.; Charushin, V. Effect of nanosized TiO_2–SiO_2 covalently modified by chiral molecules on the asymmetric Biginelli reaction. *Catal. Today* **2015**, *241*, 270–274. [CrossRef]
27. Pal, T.K.; De, D.; Senthilkumar, S.; Neogi, S.; Bharadwaj, P.K. A partially fluorinated, water-stable Cu (II)–MOF derived via transmetalation: Significant gas adsorption with high CO_2 selectivity and catalysis of Biginelli reactions. *Inorg. Chem.* **2016**, *55*, 7835–7842. [CrossRef] [PubMed]
28. Ghasemi, Z.; Orafa, F.F.; Pirouzmand, M.; Zarrini, G.; Kojanag, B.N.; Salehi, R. Zn^{2+}/MCM-41 catalyzed Biginelli reaction of heteroaryl aldehydes and evaluation of the antimicrobial activity and cytotoxicity of the pyrimidone products. *Tetrahedron Lett.* **2015**, *56*, 6393–6396. [CrossRef]
29. Moitra, D.; Ghosh, B.K.; Chandel, M.; Ghosh, N.N. Synthesis of a $BiFeO_3$ nanowirereduced graphene oxide based magnetically separable nanocatalyst and its versatile catalytic activity towards multiple organic reactions. *RSC Adv.* **2016**, *6*, 97941–97952. [CrossRef]
30. Wang, Y.; Yu, J.; Miao, Z.; Chen, R. Bifunctional primary amine-thiourea–TfOH (BPAT·TfOH) as a chiral phase-transfer catalyst: The asymmetric synthesis of dihydropyrimidines. *Org. Biomol. Chem.* **2011**, *9*, 3050–3054. [CrossRef]

31. Barbero, M.; Cadamuro, S.; Dughera, S.A. Brønsted, acid catalysed enantioselective Biginelli reaction. *Green Chem.* **2017**, *19*, 1529–1535. [CrossRef]
32. Saha, S.; Narasimha, J. Enantioselective organocatalytic Biginelli reaction: Dependence of the catalyst on sterics, hydrogen bonding, and reinforced chirality. *J. Org. Chem.* **2011**, *76*, 396–402. [CrossRef] [PubMed]
33. Khatri, C.K.; Rekunge, D.S.; Chaturbhuj, G.U. Sulfated polyborate: A new and eco-friendly catalyst for one-pot multi-component synthesis of 3, 4-dihydropyrimidin-2 (1H)-ones/thiones via Biginelli reaction. *New J. Chem.* **2016**, *40*, 10412–10417. [CrossRef]
34. Xu, G.; Wang, L.; Li, M.; Tao, M.; Zhang, W. Phosphorous acid functionalized polyacrylonitrile fibers with a polarity tunable surface micro-environment for one pot C–C and C–N bond formation reactions. *Green Chem.* **2017**, *19*, 5818–5830. [CrossRef]
35. Maurya, M.R.; Chauhan, A.; Arora, S.; Gupta, P. Triazole based oxidovanadium(V) complex supported on chloromethylated polymer and its catalytic activity for the synthesis of dihydropyrimidinones (DHPMs). *Catal. Today* **2022**, *397–399*, 3–15. [CrossRef]
36. Maurya, M.R.; Kumar, A.; Pessoa, J.C. Vanadium complexes immobilized on solid supports and their use as catalysts for oxidation and functionalization of alkanes and alkenes. *Coord. Chem. Rev.* **2011**, *255*, 2315–2344. [CrossRef]
37. Row, R.A.; Jones, M.M. Vanadium(IV)oxy(acetylacetonate). *Inorg. Synth.* **1957**, *5*, 113–116.
38. Maurya, M.R.; Kumar, A.; Ebel, M.; Rehder, D. Synthesis, characterization, reactivity, and catalytic potential of model vanadium(IV, V) complexes with benzimidazole-berived ONN donor ligands. *Inorg. Chem.* **2006**, *45*, 5924–5937. [CrossRef]
39. Ramalinga, K.; Vijayalakshmi, P.; Kaimal, T.N.B. Bismuth(III)-catalyzed synthesis of dihydropyrimidinones: Improved protocol conditions for the Biginelli reaction. *Synlett* **2001**, *6*, 863–865. [CrossRef]
40. Lu, J.; Ma, H. Iron(III)-Catalyzed Synthesis of Dihydropyrimidinones. Improved conditions for the Biginelli ceaction. *Synlett* **2000**, *1*, 63–64.
41. Zheng, S.; Jian, Y.; Xu, S.; Wu, Y.; Sun, H.; Zhang, G.; Zhang, W.; Gao, Z. N-Donor ligand activation of titanocene for the Biginelli reaction via the imine mechanism. *RSC Adv.* **2018**, *8*, 8657–8661. [CrossRef] [PubMed]
42. Guggilapu, S.D.; Prajapti, S.K.; Nagarsenkar, A.; Lalita, G.; Vegi, G.M.N.; Babu, B.N. MoO_2Cl_2 catalyzed efficient synthesis of functionalized 3,4-dihydropyrimidin-2(1H)-ones/thiones and polyhydroquinolines: Recyclability, fluorescence and biological studies. *New J. Chem.* **2016**, *40*, 838–843. [CrossRef]
43. Maurya, M.R.; Singh, D.; Tomar, R.; Gupta, P. Trinuclear cis–[$Mo^{VI}O_2$] complexes catalyzed efficient synthesis of 3,4-dihydropyrimidin-2(1H)-one based biomolecules via one-pot-three-components Biginelli reaction under solvent-free condition. *Inorg. Chim. Acta* **2022**, *532*, 120750. [CrossRef]
44. Maurya, M.R.; Kumar, N.; Maurya, S.K.; Avecilla, F. Influence of coordination geometry on the ring opening of benzoxazine: Oxidovanadium(V), dioxidomolybdenum(VI) and dioxidotungsten(VI) complexes of benzoxazine based ligands and their bio inspired catalytic applications. *Eur. J. Inorg. Chem.* **2022**, *2022*, e202200536. [CrossRef]
45. Ceson, L.A.; Day, A.R. Preparation of some benzimidazolylamino acids reactions of amino acids with o-phenylenediamines. *J. Org. Chem.* **1962**, *27*, 581–586. [CrossRef]
46. Javidi, J.; Esmaeilpour, M.; Dodeji, F.N. Immobilization of phosphomolybdic acid nanoparticles on imidazole functionalized Fe_3O_4@SiO_2: A novel and reusable nanocatalyst for one-pot synthesis of Biginelli-type 3,4-dihydro-pyrimidine-2-(1*H*)-ones/thiones under solvent-free conditions. *Rsc Adv.* **2015**, *5*, 308–315. [CrossRef]
47. Meng, F.; Shi, L.; Feng, G.; Sun, L.; Zhou, Y. Enantioselective synthesis of 3,4-dihydropyrimidin-2(1*H*)-ones through organocatalytic transfer hydrogenation of 2-hydroxypyrimidines. *J. Org. Chem.* **2019**, *84*, 4435–4442. [CrossRef]
48. Fu, N.; Yuan, Y.; Cao, Z.; Wang, S.; Wang, J.; Peppe, C. Indium(III) bromide-catalyzed preparation of dihydropyrimidinones: Improved protocol conditions for the Biginelli reaction. *Tetrahedron* **2002**, *58*, 4801–4807. [CrossRef]
49. Shaker, R.M.; Mahmoud, A.F.; Abdel-Latif, F.F. Synthesis of 2-thioxopyrido[2,3-d]pyrimidine-4-ones and 1,4-bridged bis-2-thioxo-1,2,3,4-tetrahydro-5-pyrimidine carboxylic acid ethyl ester derivatives. *Phosphorus Sulfur Silicon* **2000**, *160*, 207–222. [CrossRef]
50. Stadler, A.; Kappe, C.O. Automated library generation using sequential microwave-assisted chemistry. Application toward the Biginelli multicomponent condensation. *J. Comb. Chem.* **2001**, *3*, 624–630. [CrossRef]